Sea-Level Flight Demonstration & Altitude Characterization of a LO2 / LCH4 Based Accent Propulsion Lander

Jacob Collins [*], Eric Hurlbert [†], Kris Romig [‡], John Melcher [§]
NASA Johnson Space Center, Houston, TX 77058
Aaron Hobson [¶]
NASA White Sands Test Facility, Las Cruses, New Mexico 88012
Phil Eaton [#]
Armadillo Aerospace, Caddo Mills, TX 75135

A 1,500 lb_f thrust-class liquid oxygen (LO2) / Liquid Methane (LCH4) rocket engine was developed and tested at both sea-level and simulated altitude conditions. The engine was fabricated by Armadillo Aerospace (AA) in collaboration with NASA Johnson Space Center. Sea level testing was conducted at Armadillo Aerospace facilities at Caddo Mills, TX. Sea-level tests were conducted using both a static horizontal test bed and a vertical take-off and landing (VTOL) test bed capable of lift-off and hover-flight in low atmosphere conditions. The vertical test bed configuration is capable of throttling the engine valves to enable liftoff and hover-flight. Simulated altitude vacuum testing was conducted at NASA Johnson Space Center White Sands Test Facility (WSTF), which is capable of providing altitude simulation greater than 120,000 ft equivalent. The engine tests demonstrated ignition using two different methods, a gas-torch and a pyrotechnic igniter. Both gas torch and pyrotechnic ignition were demonstrated at both sea-level and vacuum conditions. The rocket engine was designed to be configured with three different nozzle configurations, including a dual-bell nozzle geometry. Dual-bell nozzle tests were conducted at WSTF and engine performance data was achieved at both ambient pressure and simulated altitude conditions. Dual-bell nozzle performance data was achieved over a range of altitude conditions from 90,000 ft to 50,000 ft altitude. Thrust and propellant mass flow rates were measured in the tests for specific impulse (Isp) and C* calculations.

I.Program Objectives

One objective of the Vision of Space Exploration (VSE) is to build a long term infrastructure for the human and robotic habitation of the moon and Mars. NASA is developing and evaluating technologies for liquid oxygen (LO2) and liquid methane (LCH4) propellants for possible use in this architecture. Liquid oxygen based propulsion systems will enable the use of in-situ produced propellants for lunar and Mars missions, provide higher vehicle performance, and provide commonality with breathable oxygen and fuel cell reactant storage. Not only does LO2 based propulsion benefit the VSE, but adoption of these green, or non-toxic, propellants eliminates the need to perform rigorous decontamination of the landing environment, affected lander equipment, as well as Earth-based processing facilities. In addition, the cost of the toxic propellants is ~$80 per lb_m, with LO2 based propellants costing much less than a ~$1 per lb_m. Although LO2 based propulsion is a strong contender in every trade study performed since 1964, the program's acceptance of this method of propulsion is continually plagued by a lack of flight heritage and experience. This research seeks to obtain operational experience using LO2 and LCH4 by utilizing the Armadillo Aerospace (AA) lander to demonstrate this capability.

The project was jointly funded through the NASA Innovative Partnership Program (IPP), the Propulsion and Cryogenic Advanced Development (PCAD) project, and AA. The primary objective of the partnership was to gather end-to-end operational data on a LO2-LCH4 propulsion powered vehicle in flight environments, including

[*] Aerospace Engineer, Propulsion Systems Branch - EP4, 2101 NASA Parkway, Houston, TX 77058, Member
[†] Aerospace Engineer, Propulsion Systems Branch - EP4, 2101 NASA Parkway, Houston, TX 77058
[‡] Aerospace Engineer, Systems Integration Office - EP2, 2101 NASA Parkway, Houston, TX 77058
[§] Aerospace Engineer, Propulsion Systems Branch - EP4, 2101 NASA Parkway, Houston, TX 77058, Senior Member
[¶] Mechanical Engineer, Propulsion Department - RD, 12600 NASA Road, Las Cruces, NM 88012
[#] Vice President of Operations, Armadillo Aerospace, Caddo Mills Municipal Airport Building A, Caddo Mills, TX 75135

sea level and vacuum operation. The approach utilized the strengths of each of the partners and the following actions were completed:

- Obtained ambient and altitude performance data of a modified lander engine using LO2 / LCH4 with two nozzle configurations
- Measured engine performance with a dual-bell nozzle during an altitude sweep simulating a descent profile
- Demonstrated ambient and vacuum ignition of LO2 / LCH4 ascent main engine with gas torch and pyrotechnic ignition.
- Worked towards developing a self-pressurized propulsion system to eliminate the need for GHe pressurization.

II.Armadillo Aerospace Testing Summary

A. Introduction

The AA effort evaluated three different methods of propellant pressurization, two of which eliminated the need for gaseous helium pressurization storage. The use of blow-down and self-vaporization pressurization techniques eliminated the weight and reliability concerns associated with an active pressurization methods. The utilization of the vapor pressure of cryogenic propellants benefits the vehicle design by: 1) Eliminating failure modes due to helium leakage and pressure regulator failure, or 2) Providing a redundant means to expel the propellant.

AA has a commercial interest in demonstrating the propulsion technology and their previous lander system offered a unique platform since minimal modification was required. The first flight demonstration was performed in tethered flight mode since the self-vaporization pressurizing mode demonstration resulted in lower system pressures than currently used by the AA modular vehicle. The free flying vehicle utilized self pressurization as well, but with a limited run time of only 45 seconds due to reduced performance. Figure 1 shows the vehicle in an un-tethered flight. Several technology firsts were accomplished during the program including: 1.) The first LO2 / LCH4 hot-fire test of a dual-bell nozzle at altitude while simulating a decent profile, 2.) the first LO2 / LCH4 pyrotechnic ignition at altitude, and 3.) the first self-pressurized throttling LO2 / LCH4 lander.

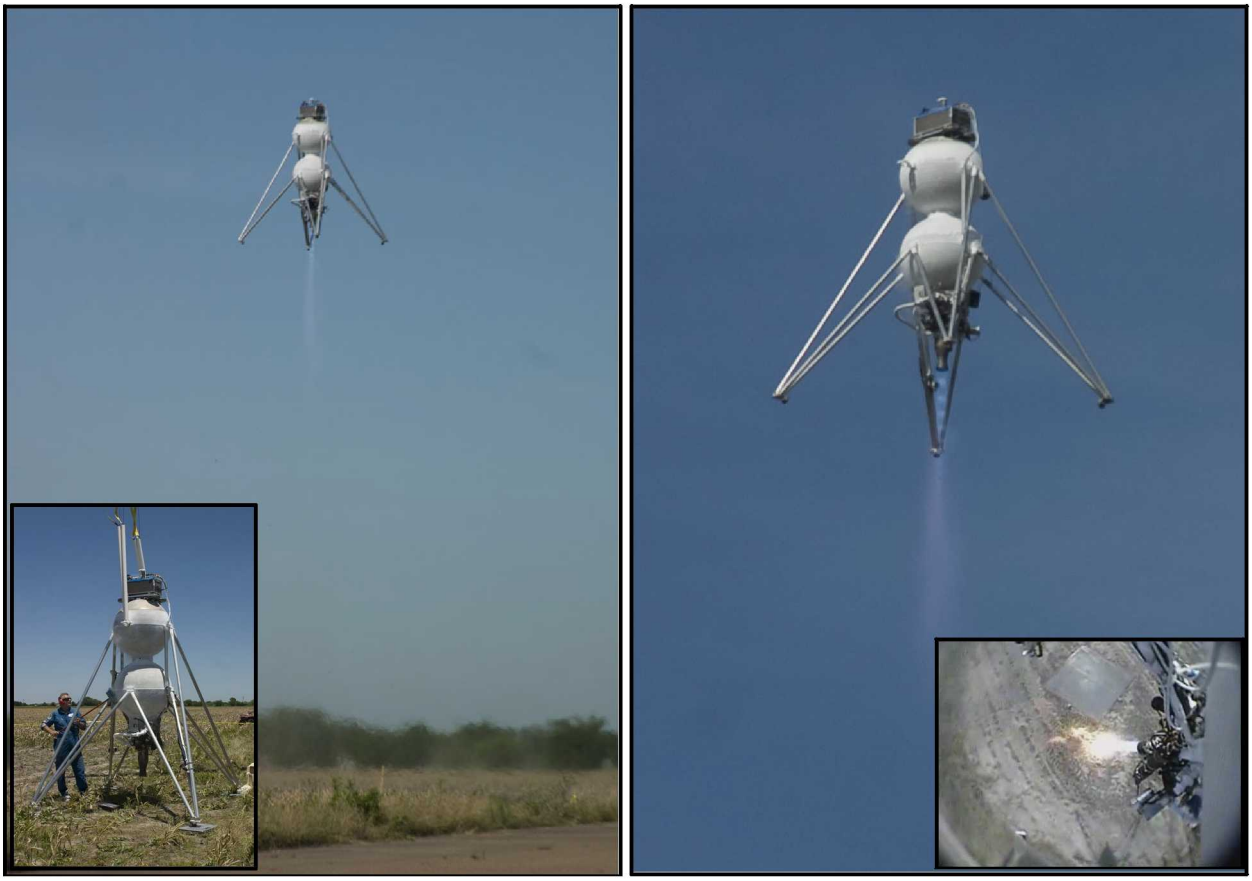

- Figure 1: Armadillo Aerospace VTOL Modular Vehicle in Typical Un-Tethered Flight Testing

B. Modification of LO2 / Ethanol Engine

AA began testing the torch igniter unit using a commercially available form of methane referred to as Department of Transportation (DOT) grade Liquefied Natural Gas (LNG). Little effort was required to convert the system for this purpose, and the appropriate mixture ratios were obtained quickly. The engine system is designed as a pressure-fed propulsion system for a Vertical Take Off and Landing (VTOL) vehicle that can be utilized for sub-orbital flights. The AA assembly is constructed of 304, 310, and 316 Stainless Steel. The welded subassemblies that make up the AA engine consist of the injector, the chamber, oxidizer (LO2) and fuel propellant inlets, and the torch igniter (also pyrotechnic igniter).

The torch igniter system is welded to the chamber assembly and consists of a square-tube igniter chamber fed by gaseous oxygen and methane. The torch igniter generates a flame by using a spark ignition source to ignite the gaseous oxygen (GOx) / gaseous methane (GM) mixture in order to ignite the propellant mixture in the engine chamber. The torch igniter was installed on the baseline engine design and ran for just over 10 seconds at full throttle without any damage to the rocket engine or igniter body.

The Armadillo engine injector design had worked well with LO2 Ethanol designs for short duration runs less than 60 seconds. Over 60 seconds, and the recirculation of hot combustion gases would begin to degrade the face and upper chamber wall.

C. Design Progression

As a prelude to design considerations for the LO2 Methane combination, the AA team began to modify the all steel engine for long duration runs using LO2 Ethanol with the intent to modify the design after all of the thermal recirculation problems were solved. A Fuel-Ox-Ox-Fuel (FOOF) injector was designed and adjusted to accommodate the appropriate mixture ratios for the high purity LO2 / LCH4.

AA took delivery of the first load of High Purity Methane (LCH4) and was subsequent testing uncovered problems including non-ignition events, leaks, chugging, and high frequency instabilities. The team varied the orifice ratios, tank pressures, feed system configuration, and even reverted to the first injector that was run to verify operations.

First, it was discovered that the DOT grade LNG had "impurities" up to 3% that completely changed the ignition characteristics of the propellant combination resulting in intermittent torch igniter non-ignitions. The datasheets available for LNG revealed that the Ethane, Propane, and Butane components of the LNG had the effect of increasing the combustion range of the fuel.

Second, it was discovered that when the main propellant mixture was running extremely fuel rich, the combustion was somewhat stable regardless of the injector impingement style. When the mixture ratios were brought into a range that gave a reasonable specific impulse (Isp), the unlike impingement schemes such as ox-fuel-ox (OFO), or FOOF would run smooth only at full throttle. When the engines were throttled back for operation on a lander, the engines would suffer an extreme oscillation in the 9000Hz range that would vibrate loose all of the Swagelok fittings on the engine and mechanically fail the sparkplugs.

After repeated tests to try and reduce the oscillations in the combustion, AA moved to a like impinging pattern to regain combustion stability at the expense of performance. The engine stability was sufficient across the throttling range, but a significant amount of L* was required to be added to the chamber (the diameter was fixed so length must be added). The final impingement pattern was fuel-fuel (FF) ox-ox (OO) OO FF from inside to outside. The chamber wall is cooled by an annular ring of fuel elements.

The measured system level Isp for a 60 second flight is approximately 148 seconds at an altitude of 560 feet Mean Sea Level (MSL). This includes all ignition and shut down sequences through the entire flight at all throttle positions and chamber pressures.

D. Design Results

The vehicle AA placed the engine on for tethered and un-tethered testing was the VTOL Modular Vehicle. Figure 2 represents test data from the first pyrotechnic ignition on a tethered flight using LO2-LCH4 on a 1,500 lb_f class engine. Propellant run tank pressures, igniter and chamber pressure, manifold pressures, and main valve commands are shown. Figure 3 shows the vehicle running LO2 / LCH4 in a tethered flight test using a pyrotechnic ignition. Figures 4 represents similar data measured from a static horizontal test. Figure 5 shows the engine on the horizontal test sled at full throttle.

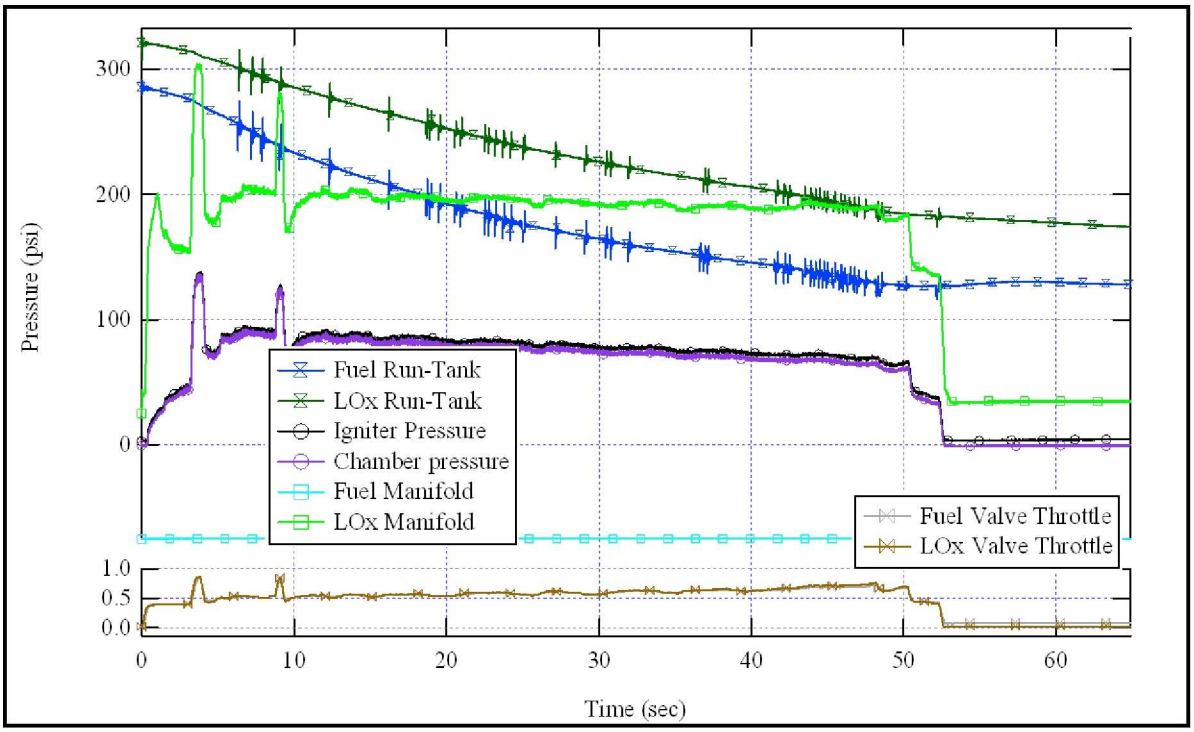

Figure 2: Vertical Take-off and Landing (VTOL) test data during tethered flight, first pyrotechnic ignition demonstration test for VTOL

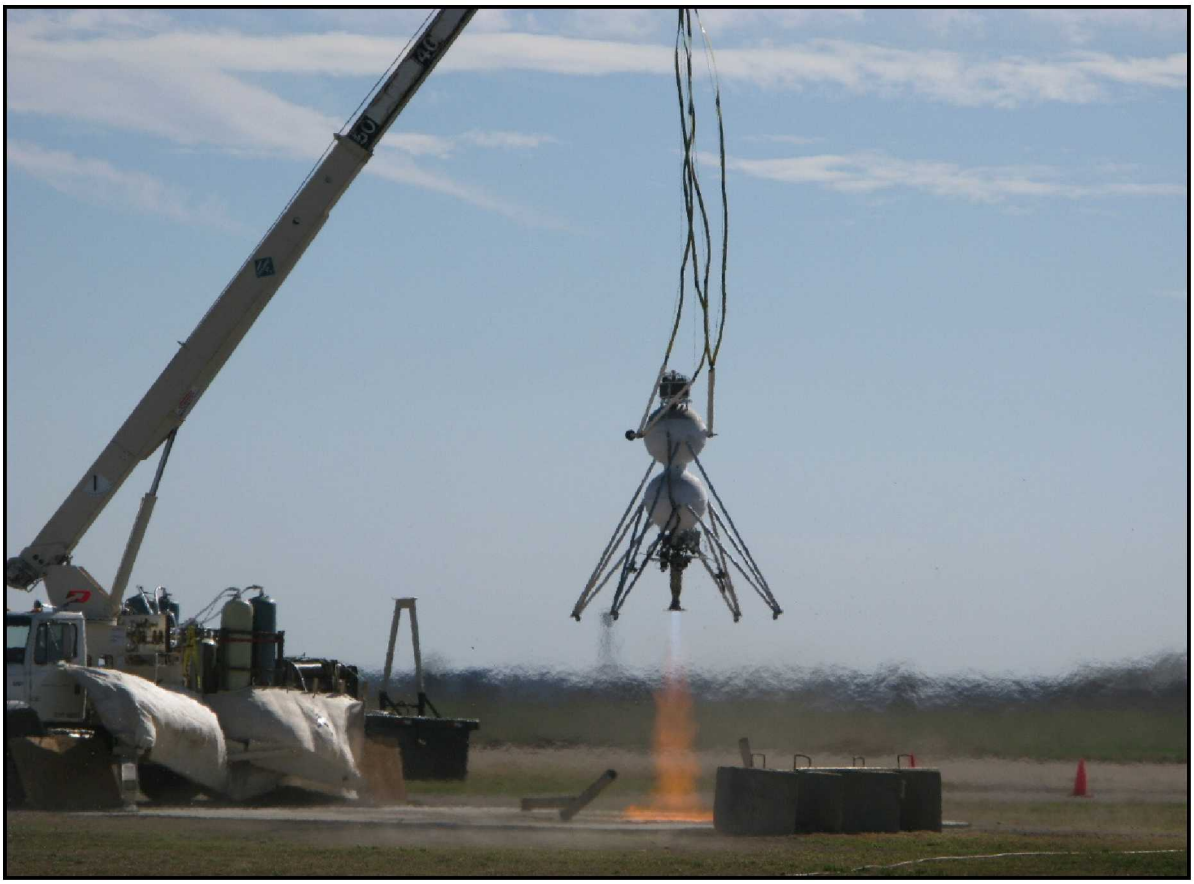

Figure 3: Armadillo Aerospace VTOL Modular Vehicle in Typical Tethered Flight Testing, pyrotechnic ignition

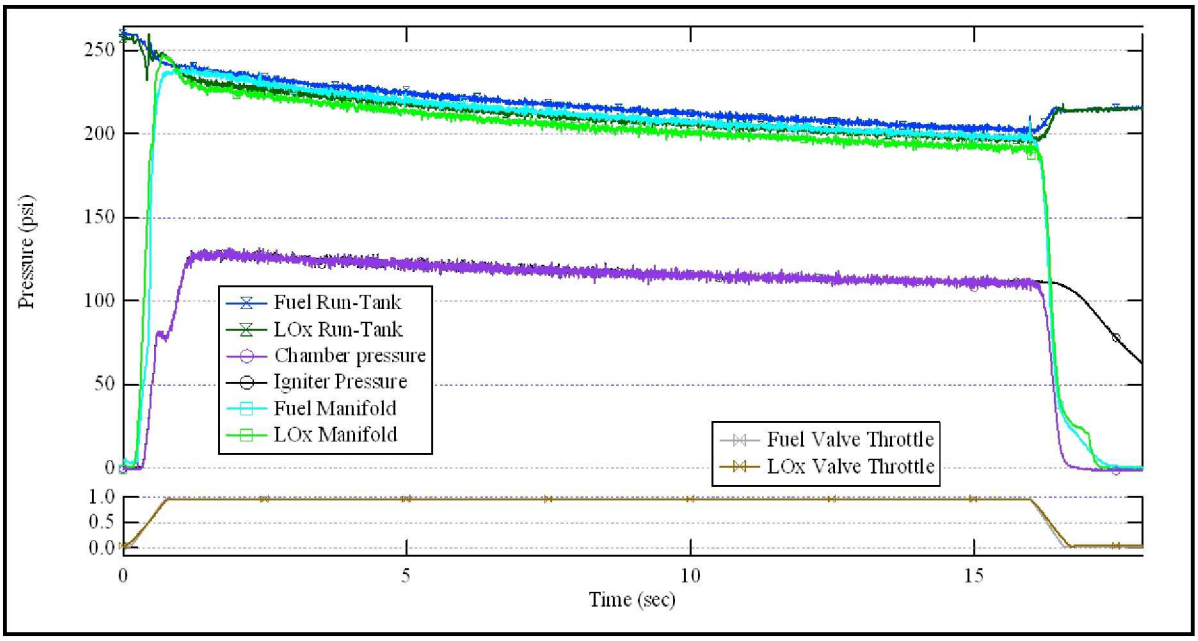

Figure 4: Test data from static horizontal test, first pyrotechnic ignition demonstration in horizontal test sled

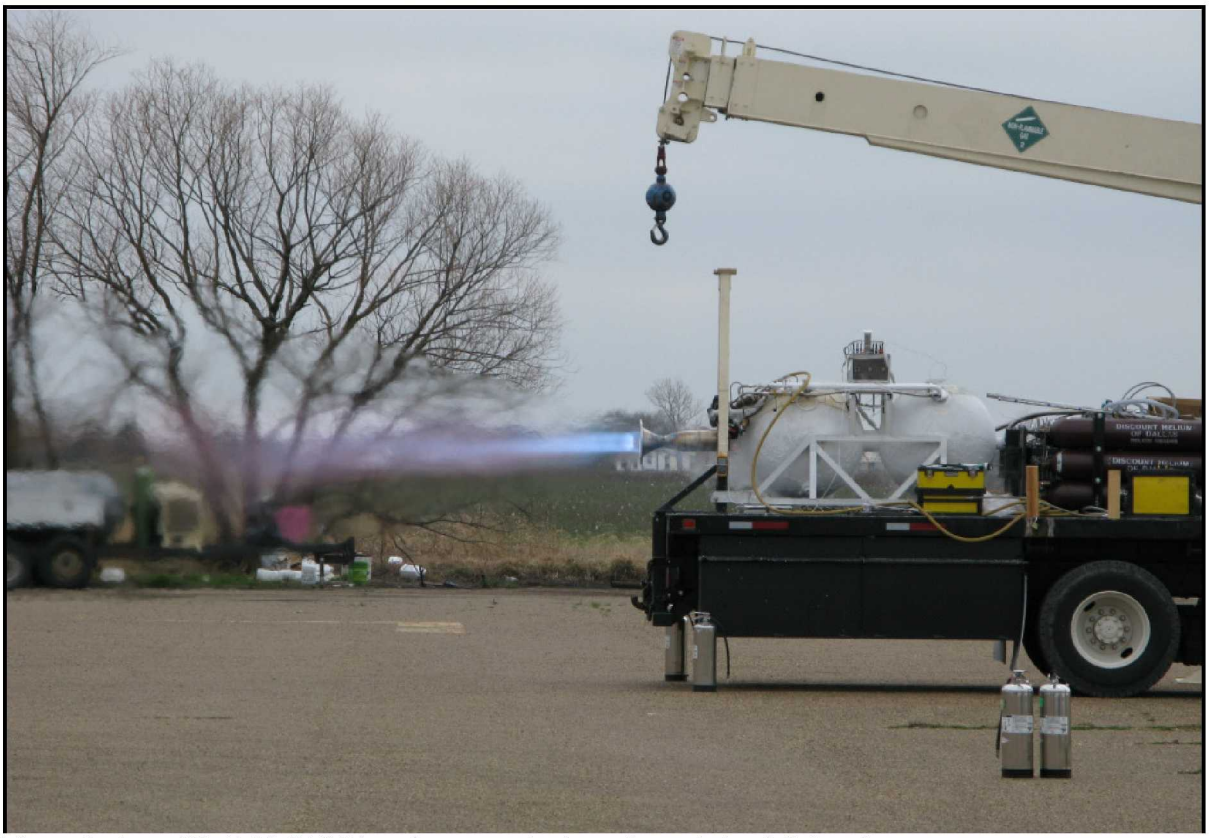
Figure 5: Armadillo LO2 / LCH4 engine test on horizontal test sled at full throttle

E. Nozzle Summary

1. Nozzle Overview

The objective of the altitude testing at WSTF was to measure the engine performance using two different bell nozzle configurations. The two nozzles designed were a Rao-optimized, and dual-bell nozzle. Unfortunately, the

Rao optimized nozzle was not tested at WSTF due to schedule and budgetary constraints. However, the design methodology is described below.

The Rao-optimized nozzle optimizes maximum thrust performance for a given length and contour using a variation optimization method based on Lagrange multipliers. However, significant performance losses are induced during the off-design operation of nozzles when the flow is over-expanded during low altitude operation (ambient pressures higher than the nozzle exit pressure), or under-expanded during high-altitude operation (ambient pressures lower than the nozzle exit pressure).[3]

Slight overexpansion merely causes a slight reduction in efficiency. However, if the pressure is approximately 2.5 times lower than ambient then flow separation occurs. This can cause jet instabilities and damage the nozzle or cause control difficulties of the vehicle. The exact prediction of the flow separation point has not yet been fully solved and is the subject of ongoing research.[4]

At sea-level operation, the pressure within the separated flow region of the dual-bell nozzle extension is slightly below the ambient pressure, inducing a thrust loss, the aspiration drag. In addition, the flow transition from the sea-level mode to the altitude mode occurs before the optimum crossover point, which leads to a thrust loss compared with an ideal switchover. The non-optimum contour of the full-flowing dual-bell nozzle in the altitude mode results in further losses. Despite these additional losses, the dual-bell nozzle provides a significant net impulse gain over the entire trajectory.[7] In low altitudes, controlled and symmetrical flow separation occurs at the wall inflection, which results in a smaller effective area ratio without generating dangerous side loads. In higher altitudes, the nozzle flow is attached to the wall until the exit plane and the full geometric area is used. Due to the high area ratio, better performance is achieved in a vacuum. [5]

Despite the increased performance, a flight program would require a trade study to be performed over the weight increase of the dual-bell nozzle versus its performance increase.

2. Nozzle Constraints

Both the Rao-optimized and dual-bell configurations were designed with an 18 inch length constraint and a 3.5 inch diameter throat. The length constraint is due to the AA flight vehicle design of the landing gear. Better performance, particularly with the dual-bell nozzle is predicted with a longer nozzle.

The vehicle trajectory was assumed to lift off at 5,000 ft ("sea level" in New Mexico's WSTF), have 300 psi chamber pressure, and provide continuous thrust up to 70,000 ft and then coast to 100,000 ft. At 70,000 ft, the chamber pressure was expected to decrease to approximately 225 psi (pressure feed engine). In actuality, the location for liftoff may not be 5,000 ft and the engine may not shut off at 70,000 ft. However, the nozzle contour was designed with the 100,000 ft altitude constraint in order to test engine performance at lower ambient pressures.

The nozzles were designed with an initial chamber pressure of 300 psi. However, while the nozzles were being fabricated, AA selected a lower chamber pressure to be tested in order to simulate the conditions of a self-pressurized swirl type injector currently in development. Therefore, slightly higher thrust could be achieved.

3. Nozzle Design

The nozzle thickness was selected by matching the thickness of the existing AA engine design. The safety of this thickness was verified by modeling the nozzle throat as a thin-walled cylinder and using hoop stress calculations to determine the minimum thickness. The values used are based on the Two Dimensional Kinetics (TDK) software's prediction of the maximum temperature and pressure at the throat.

In addition, a Proe Mechanica analysis was performed to measure the effects of an asymmetric pressure load of 10 psi in 8" diameter circle projected onto the inner surface of bell. 10 psi was selected as a conservative maximum pressure in the event of a major problem based on TDK predictions and a chamber pressure (Pc) of 300 psi (actual Pc used in testing was ~150 psi). Figure 6 below shows a maximum deflection of .040" (lower far right) in a 24.0" diameter nozzle and the maximum stress to be approximately 44 ksi (at lower right around screw holes in nozzle flange). This amount of stress is not a concern at the screw holes and the average stress (light blue and dark blue regions), is not sufficient (~5,800 psi). Therefore it was determined that the side loads generated will not be an issue inside the WSTF test chamber.

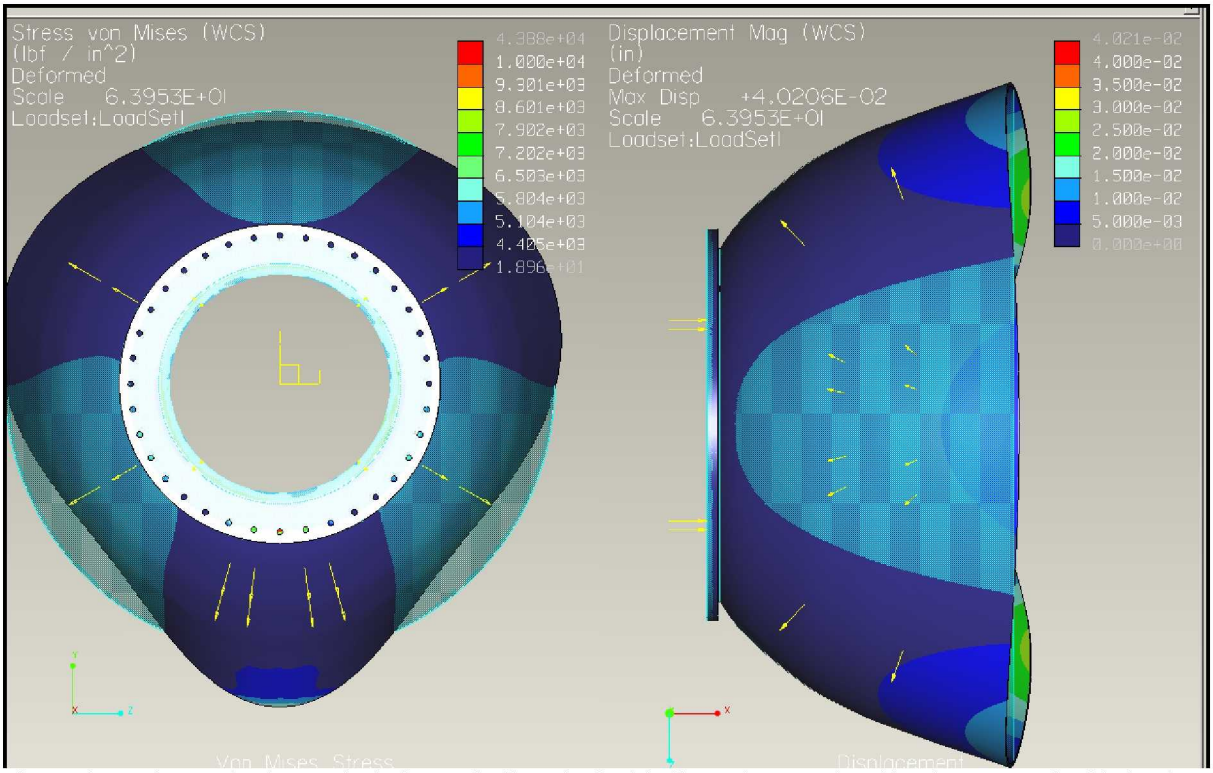

Figure 6: Pro/E Mechanica analysis form of effects in dual-bell nozzle assuming 10 psi asymmetric side load

In order to decrease the turnaround time between test runs at WSTF, the nozzles were designed in three sections. Section 1 was welded directly to the engine. Nozzle attachments 2 or 3 can be interchanged by bolting (flange mated) directly to section 1 using 36 x ½ inch thru holes. The flanges are separated by a 0.031" thick GRAFOIL (flat foil reinforced graphite) gasket. This allows the nozzle attachments to be interchanged quickly opposed to welding or changing the engine out. Figure 7 shows a Pro/E depiction of the section 1, 2, and 3 nozzle attachments and Figure 8 represents the two nozzle configurations installed on the thrust chamber.

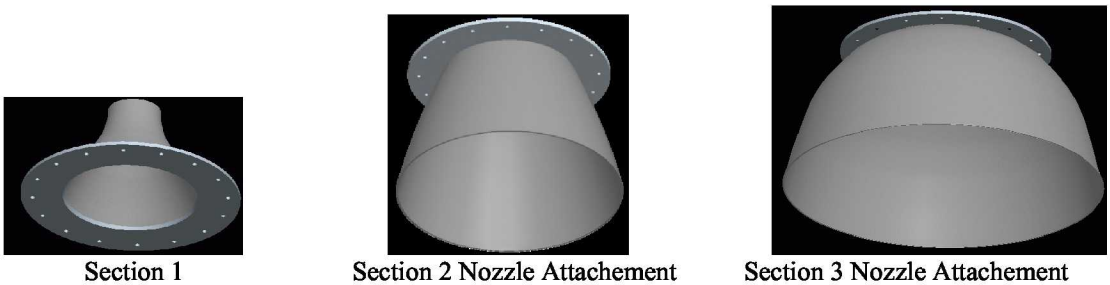
Section 1 Section 2 Nozzle Attachement Section 3 Nozzle Attachement

Figure 7: Armadillo Aerospace Nozzle Attachments

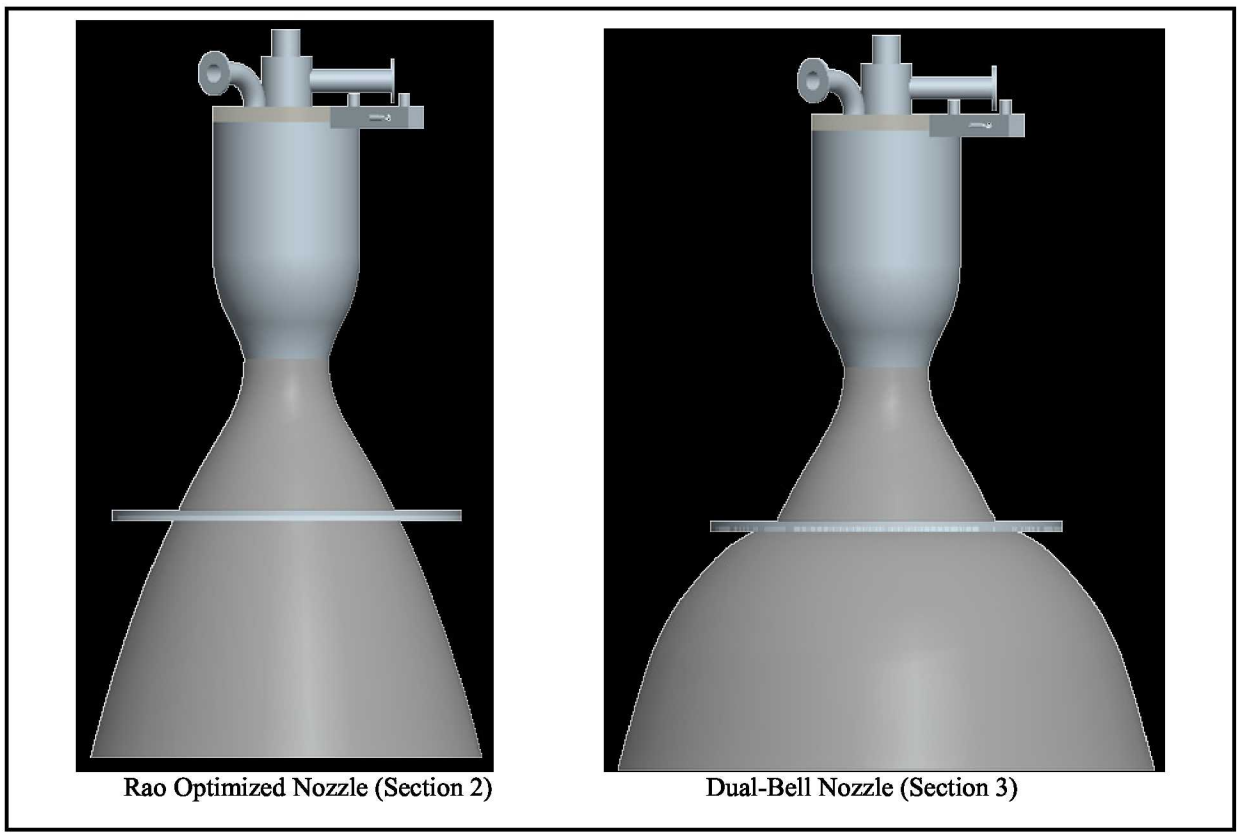

Figure 8: Thrust Chamber with Section 1 and Section 2 or 3 Attachment

III.WSTF Test Setup Summary

A. Introduction

To benefit AA's commercialization activities and provide NASA with engine concept data after the successful sea level tethered testing, a NASA WSTF test facility was modified to perform altitude characterization tests on the modified AA LO2-LCH4 engine. The objective of the WSTF hot-fire testing was to measure engine performance during a static hot-fire in a simulated altitude environment. The Armadillo Aerospace Main Engine (AAME) was installed on the Auxiliary Propulsion System Test Bed (APSTB) at Test Stand 401 using the Small Altitude Simulation System (SASS) to simulate the altitude environment.

B. Test Stand

The APSTB consists of two 550 gallon cryogenic tanks supplied with vacuum jacketed feed-lines. The LO2 tank is pressurized using facility GN2 and the methane tank is pressurized with facility helium. The AAME manifold is supplied from the APSTB through an auxiliary feed-line that connects to the propellant run tanks. The AAME is installed directly underneath the APSTB and connects to a modified bayonet assembly shown in Figure 9 below.

Bleed valves were used to ensure liquid conditions at the main valve inlets prior to beginning a test profile. A GN_2 purge was required downstream of the main valve to purge injector passages before and after tests. Solenoid valves used for engine purges during previous hot-fire testing on the APSTB were used to support this requirement.

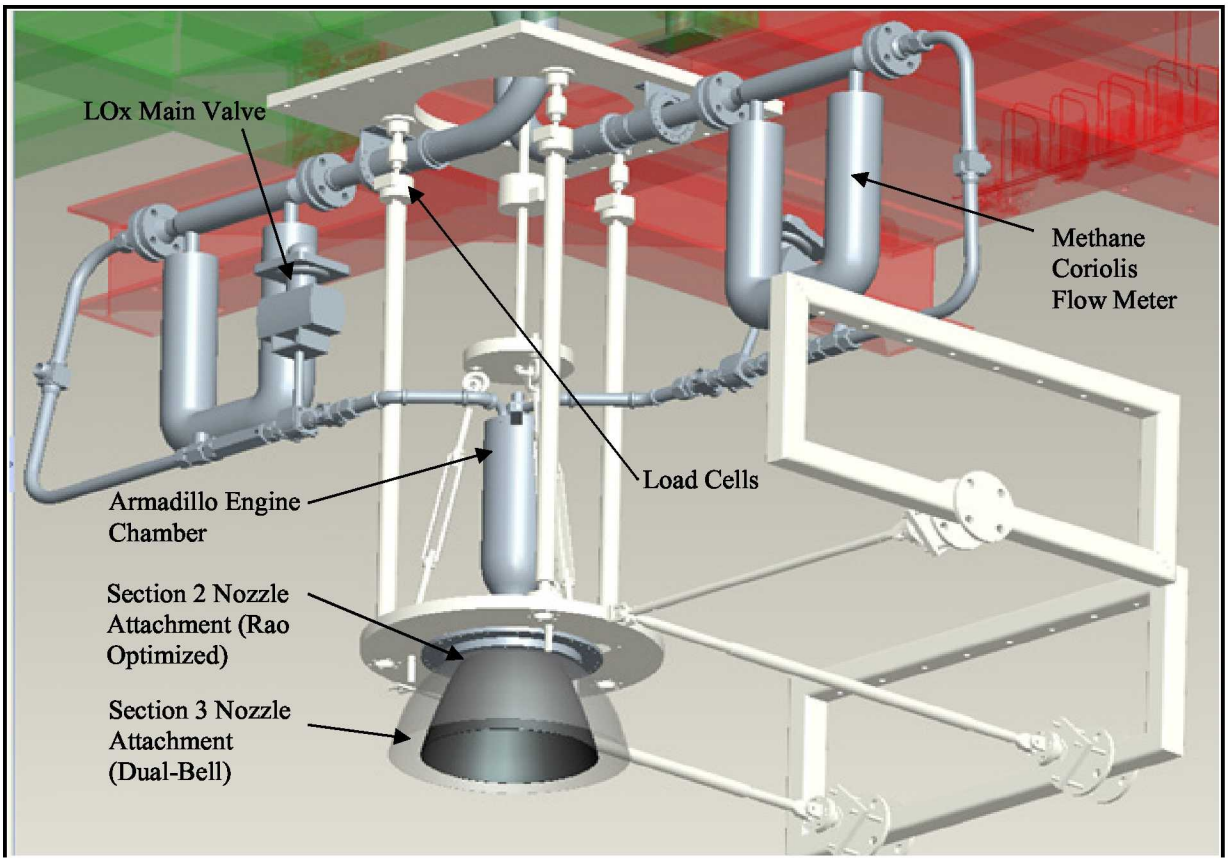

Figure 9: AA Engine Installed on the APSTB, dual-bell and RAO-optimized nozzles attachments shown overlaid

4. Thrust measurement system

After the test article, manifolds, and other support lines and cables were installed, the thrust measurement system was characterized through a series of pull and hammer impact tests. The system's thrust calibration characteristics as well as natural frequencies were measured and documented. It is important to note that no nozzle extensions were installed during this characterization and the additional weight may result in slight differences in the frequency response of the structure. In addition, the initial characterization was performed at ambient temperature and pressure, which also may have an effect on the system thrust calibration and frequency response.

Engine thrust was measured by summing three 2,000 lb_f dual bridge load cells. At a minimum, a routine calibration of the thrust measurement system was performed prior to each test day. To help mitigate for temperature and pressure differences, thrust calibration data was gathered before or after hot-fire tests to ensure that the conditions during the calibration data are as close as possible to the actual test conditions. The system was calibrated by applying loads with a pneumatic load cylinder to a 10,000 lb_f calibrated load cell. The calibration data was analyzed post test by performing procedural steps on each pre-test calibrated run with its associated hot-fire in order to increase the force measurement accuracy.

5. Accelerometer

Armadillo Main Engine stability monitoring uses three accelerometers with a frequency of 500-5,000 Hz. The accelerometer block was attached to the top face of the injector plate. AA did not measure frequency during sea-level tests, and therefore did not have predicted cutoff amplitudes for the Stability Cutoff System during WSTF tests. Therefore, the hot-fire tests were at first limited to 5 seconds until accelerometer data was evaluated for stability cut-off amplitudes.

The thrust stand natural and resonant frequency was determined before test initiation through a thrust stand characterization. This involves tapping the thrust stand with a hammer while monitoring the frequency and allows for a quick troubleshooting of an engine or a thrust stand problem.

6. Flow measurement

Both coriolis and turbine flow meters were used in series to provide redundant flow measurement. Temperature and pressure data was collected near the flow meters so that mass flow and density can be calculated posttest. Both

flow rate techniques were compared to each other and produced accurate results. The real-time flow, C*, and Isp results were calculated using the turbine flow meters in combination with Reference Fluid Thermodynamic and Transport Properties (REFPROP) software (version 8.0) for calculation of density.

The coriolis flowmeter is a 2" Micro Motion ELITE sensor using a multivariable flow and density transmitter MVD 2500. Unlike traditional flow measuring techniques, coriolis meters respond directly to mass flow without regard to inlet flow conditioning (i.e. straight runs of tubing). The accuracy of the system is 0.05% of the flow rate with minimal pressure losses. The limitation of this instrument is that the system must be at steady state before reliable data becomes available. The time to reach this state varies from test to test but values as long as 10 seconds have been observed. Though the coriolis flowmeter is not functional during the initial transient data, for long duration runs the data is precise. Figure 10 represents a comparison of the coriolis and turbine flow meters.

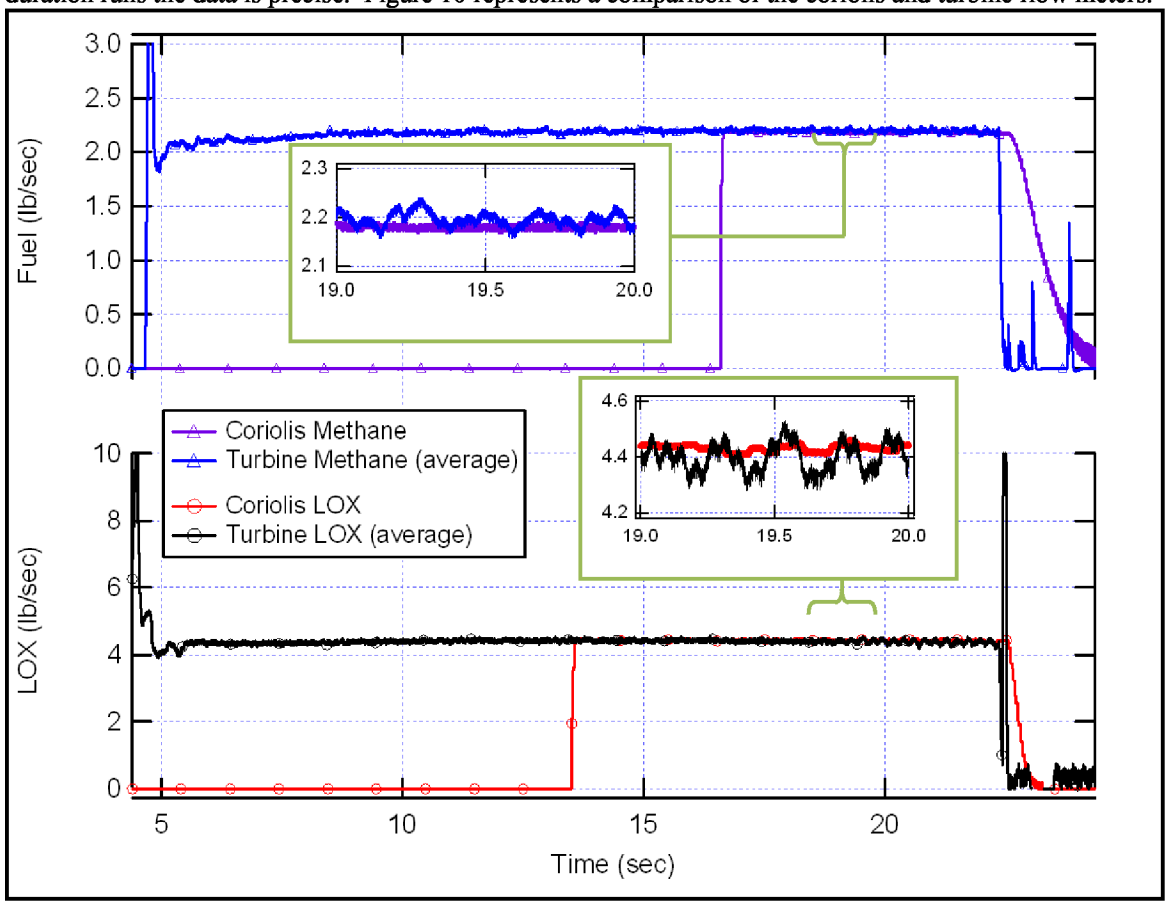

Figure 10: Hot-fire 10 Plot: Coriolis versus Turbine Flow Meter Comparison

The turbine flowmeter is a Hoffer HO liquid turbine series flow-meter using a CAT3 Microprocessor Controlled Transmitter. The instrument has an accuracy of + 0.5% over the flow range of 8-130 GPM. The limitations of the instrument are 150% of maximum flow over range (over spinning the rotor) which can occur at startup before the feed lines are chilled in. In addition, straight runs of tubing (10 diameters of the nominal turbine meter inlet size upstream and 5 diameters downstream) are required into and out of the flowmeter to assure the flowing stream's velocity profile is symmetrical.

7. Instrumentation

Pressure transducers for the engine chamber pressure (Pc) and igniter pressure (PCIGN) were mounted near the engine and attached to the engine sense-ports using ~12" lengths of 1/8" tubing. Type K thermocouples were used to monitor hotspots on the engine and extension sections. Thirty six thermocouples were tack-welded to all segments of the AA engine assembly, including nine on each of the following areas: the AA engine, Section 1, Section 2, and Section 3 nozzle extensions. On the AA engine, three thermocouples (TENG1-3) were attached just below the injector plate at 120° intervals around the chamber, three thermocouples (TENG 4-6) were attached at the middle of the chamber at 120° intervals, and three thermocouples (TENG7-9) were attached at the throat in 120° intervals. On the section 1 nozzle, nine thermocouples (TCAHMB1-9) were attached in a linear pattern approximately 0.7" apart.

Nozzle Section 2 (RAO-optimized) had nine thermocouples attached in a linear pattern approximately every 1.2". Nozzle Section 3 (dual-bell) had nine thermocouples attached in the same pattern as the RAO nozzle, but due to the increased curvature, each thermocouple has slightly greater straight-line distance between each other. Both Section 2 and 3 used the nomenclature TCHAMBEXT1-9 (never used at same time).

Redline limits were placed on the thermocouples near the throat of the AA engine and included logic to prevent a single off-scale high thermocouple (indicative of a thermocouple weld failure) from causing a shutdown. These thermocouples were used to monitor the exhaust gas flow characteristics and are shown below in Figures 11 and 12. Figures 13 and 14 represent the AAME installed in WSTF Test Cell 401.

Figure 11: Dual-Bell Nozzle Thermocouples

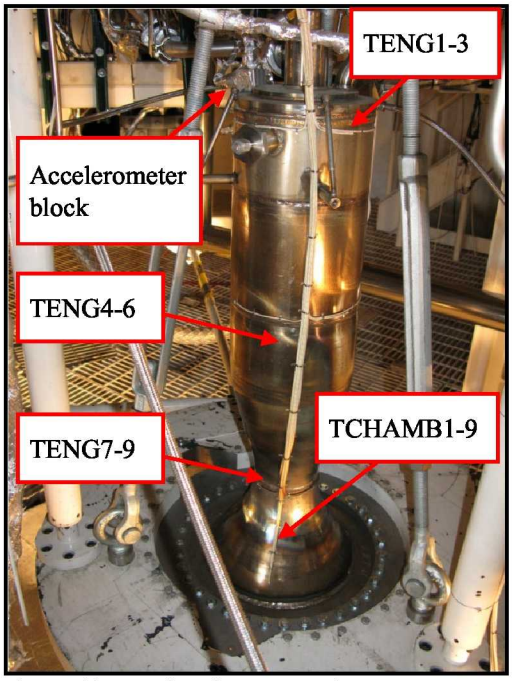

Figure 12: Engine thermocouples

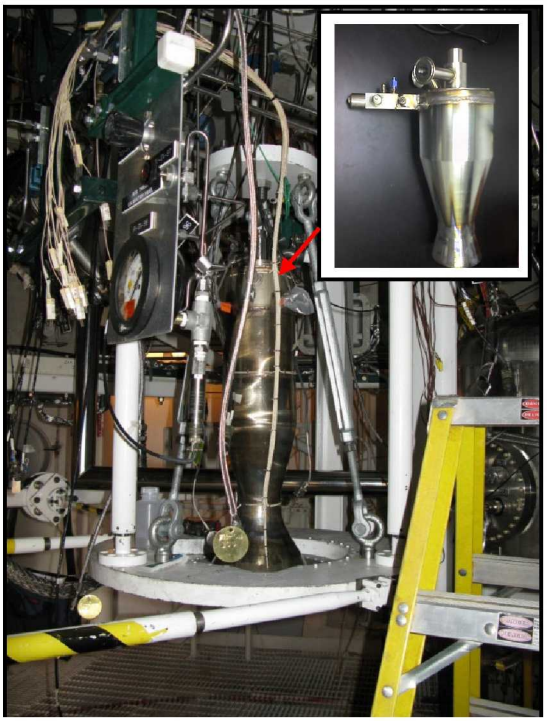

Figure 13: AAME Installed

Figure 14: AAME with Dual-Bell Installed

8. Ignition Systems

For the WSTF testing, there were two igniters positioned on the engine chamber at 180 degrees from each other including a gas torch igniter system and a pyrotechnic igniter. Both, ignition systems were tested at ambient and vacuum environmental conditions during the hot-fire testing. Gaseous methane and oxygen are available through mobile carts of standard gas K-bottles positioned outside Test Stand 401. A Unison Exciter, model 59501-500700-1 rev B SN 0000001 was installed next to the Armadillo engine to provide energy to the spark-plug. This exciter has a proven record at vacuum conditions and has been used during previous PCAD test programs.

The pyrotechnic igniter system consisted of a J2-X gas generator pyrotechnic igniter, supplied by Pacific Scientific Energetic Materials Corp. The J2-X pyro igniter is fired using a NASA Standard Initiator (NSI), which is electrically controlled with a NASA Pyrotechnic Initiator Controller (PIC).

IV. WSTF Testing Summary

The AAME test system was utilized between April 3rd and April 17th for 28 cold flows, 19 torch igniter tests, and 10 hot-fire tests. Hot-fire tests # 1-7 were conducted at ambient atmospheric pressures using two different nozzle configurations. The nozzles tested were the Section 1 nozzle (1:7.7 expansion ratio) and the Section 3 dual-bell nozzle extension (1:46 expansion ratio). Hot-fire tests # 8-10 were performed at simulated altitude conditions using the dual-bell nozzle extension. Due to scheduling constraints and inability to use the Large Altitude Simulation System (LASS), full duration tests were not achieved and the Section 2 nozzle extension (Rao optimized) was not used.

A. Cold Flow Testing

After standard cryogenic shock and leak tests were performed on the test article, cold flow testing was conducted. Liquid nitrogen was used in place of liquid methane in order to mitigate risks involved with releasing large quantities of methane propellant inside the test chamber. A one second cold-flow duration was used for the first test of each propellant to ensure that catch-pan placement, and vapor dispersion was adequate. All subsequent tests were 5 second durations.

B. Igniter Testing

Torch igniter testing at ambient pressure conditions inside the test stand were to determine the proper settings for the k-bottle supply pressures to the torch system, and to assess PCIGN for healthy ignition. AA performed extensive torch-igniter testing of their system and found that reliable ignition occurs when the run-tanks of their vehicle are at equal pressures. To match Armadillo Aerospace's igniter performance, pressures were adjusted on the k-bottle supply.

Torch igniter testing at simulated altitude conditions was then performed. The SASS was used to pull vacuum on the cell. The testing indicated that in altitude conditions, PCIGN climbs to ~24 psia with the GOx supply set to 375 psig and the GM supply set to 215 psig and was repeatable. The pyrotechnic ignition system was validated by performing a hot-fire of an NSI inside the test stand.

C. Hot-Fire Summary

1. Hot-Fire 1

The first series of hot-fire tests (1 to 4) were performed at ambient pressures with the Section 1 nozzle installed (no nozzle extensions). Hot-fire 1 was sequence profile-inhibited due to gas torch igniter operations.

2. Hot-Fire 2

Hot-fire 2 was the first successful ignition at WSTF and ran to completion through the 5-second test profile. A pre-start fire-ball was also seen during this hot-fire test just before main engine ignition. Figure 15 shows the plume shape and color during hot-fire 2, showing the exhaust gas contracting at the exit of the nozzle indicating overexpansion.

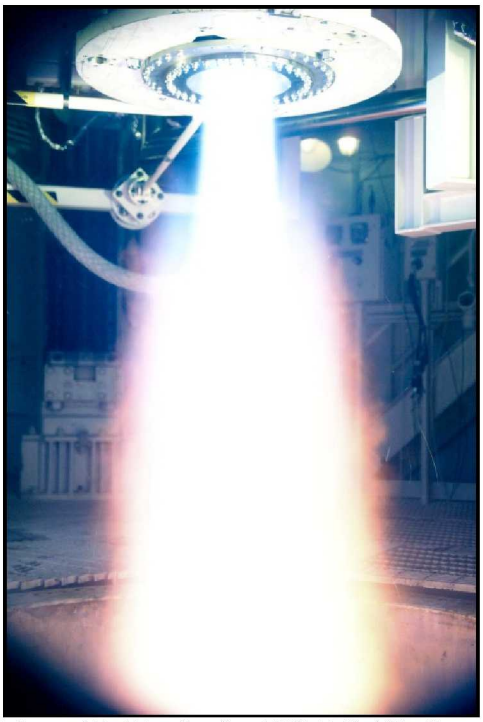

Figure 15: Hot-fire 2 at WST TS-401, first successful test of the Armadillo engine at WSTF, gas-torch ignition, Section 1 nozzle installed only, ambient altitude conditions

3. Hot-Fire 3

Hot-fire 3 performed the same 5 second profile but with a lower target MR. This was achieved by lowering the run-tank set-pressures. A small fire-ball similar to that seen in the previous tests was viewed during start-up, but there was also a larger fireball which appeared to occur in the altitude diffuser duct at approximately +1 second into test. This appears as a large orange flame which filled the diffuser and "blew-back" up toward the engine. After 1 second the plume stabilizes to a narrow blue flame similar to that seen from hot-fire 2. Post test analysis shows that the LO2 system had flow oscillations in the LO2 manifold at 1+1.5s. This can be seen in the flow meter (Figure 10), temperature, and pressure data. The flow oscillations do not appear to be related to the initial orange flame observed and are not readily apparent from review of video. One hypothesis to explain the flow oscillations is that they represent gas bubbles in the manifold which temporarily allowed faster flow velocities in the manifold. As with hot-fire 2, the plume is smaller than the exit diameter of the nozzle indicating over-expansion.

4. Hot-Fire 4

Hot-fire 4 performed the same test profile but with lower run-tank set-points in order to simulate lower MR than achieved in the previous tests. The run-tank set-points were lowered and the LO2 temperature control loop was changed in order to conserve propellant during the bleed valve cycling (the bleed valve was not able to keep the temperature of the LO2 at full saturated temperatures at the reduced pressures). The reduced pressures did not provide enough flow through the bleed valves because the liquid was flashing to gas in the bleed lines and providing too much back pressure. This was not the case for the methane because the lower density of the methane did not require as large a bleed line at that same pressure.

Ignition was achieved this time with a large orange fire-ball occurring at start-up around the engine nozzle. This died down after about 1.5 seconds and the plume narrowed to a small blue flame. Compared to the previous tests, the plume was shorter and narrower and sputtered, appearing almost to go out temporarily. After the engine valves came closed, some residual orange fire-balls were observed as un-burnt propellant was consumed outside the engine chamber. Overall, the average engine performance is extremely low. As with hot-fire 3, the LO2 turbine flow meter showed unsteady flow oscillations. A large flow spike occurs at T+2 seconds with another spike occurring at T+4.5 seconds. As with hot-fire 3, these may indicate sudden increases in flow velocity that are a result of two-phase or vapor flow. It is interesting to note that the methane flow rates for both hot-fire 3 and 4 remains steady and it was only the LO2 side that showed unsteady characteristics. The plume for hot-fire 4 was very thin and short, and also shows evidence of nozzle over-expansion

5. Hot-Fires 1 to 4 End Day Summary

Daily inspection revealed no damage to engine. The only visible sign that there was fire was that the caution stickers on the horizontal stabilizers were singed. Probably the best sign that the flame temperature was cool was that the paint on the bottom of the thrust ring is intact. The accelerometer block coupling failed and no significant accelerometer data was measured.

6. Hot-Fire 5, 6, and 7

The second series of hot-fire tests (5 to 7) was also performed at ambient cell pressures, but with a new nozzle configuration. The dual-bell nozzle which expands out from the nozzle throat at a ratio of 46:1 was installed. At ambient pressure conditions, this nozzle did not change the engine performance due to the exhaust gas flow separating from the Section 1 nozzle. The intent for testing this nozzle at ambient was to get a baseline data point with this nozzle configuration before going to altitude testing. Three hot-fire tests were performed, each with increasing run-tank set-pressures to measure engine performance with higher MRs.

To help mitigate the orange fireballs observed at the start of the previous tests, the profile start sequence was modified to remove the cycling of the main fuel valve to reduce the amount of un-burnt propellant put into the test cell prior to ignition. To compensate for the loss of injector chill time, the LO2 main valve was cycled for twice as long.

Hot-fire 5 achieved stable ignition. An orange fireball was observed during the initial start-up but not to the extent that was seen previously. Due to the installation of the dual-bell nozzle extension, the exit plane to the Section 1 nozzle was not clearly visible and therefore difficult to determine plume expansion characteristics.

Hot-fire 6 and 7 achieved stable ignition.

7. Hot-Fire 8

Hot-fire 8 was conducted with simulated altitude conditions using SASS and with the Dual-bell nozzle extension installed on the test article. Calculations from the altitude group indicated that the SASS would not have sufficient pumping power to maintain vacuum pressure in the cell when the engine fired. While steady-state engine performance characteristics and long-duration engine firings could not be achieved with SASS, the altitude sweep (simulated decent profile) was accomplished.

In order to protect the test stand and facility hardware, the test stand ambient temperatures were monitored for temperatures above 300°F the vacuum line for temperatures above 1000°F (design limit of the shutter valve). To help provide cooling to the test cell, the GN2 break valve was opened to provide 1 lb/s of flow into the test-cell during the engine firing. This flow helps provide convective cooling in the test cell as well as assists in carrying stray propellant toward the diffuser exit. This valve was actuated manually about 15 second prior to initiating the firing sequence.

Due to limitations of SASS, a low engine performance target Pc was chosen and run-tank pressures were set to 150 psia each. The engine was armed with the J-2X pyrotechnic initiator to use for the first hot-fire attempt, with the gas-torch igniter system set-up as a back-up. The engine achieved ignition with the J-2X pyrotechnic igniter at a test-cell pressure of 13 Torr, equivalent to about 90,000 ft altitude.

On ignition a large fireball occurred outside the engine chamber. This flame appeared yellow-orange, was observed filling up the test-cell, reaching as high as the top of the run-tanks of the APSTB, and persisted approximately 2 seconds into the test. After the start-up transient, the engine plume was observed as a blue-white stream with a shock a few feet under the nozzle. The plume appears slightly under-expanded in the dual-bell nozzle. As the pressure in the cell increased, the shock moved closer to the nozzle. The test was halted at approximately 5 seconds when test cell temperatures which had climbed to 350°F.

The start-up transient exhibited a high-acceleration event when compared to those seen during ambient pressure firings, causing damage to the test system. Some pressure transducers received zero offsets from dynamic effects which occurred. The thrust measurement load-cells also were damaged. This indicates that the thrust stand was subjected to a momentary force beyond 1.5 times the load cells, possibly as high as 9000 lb_f.

The post-test system walk-down found that the spark-plug had been broken from the torch-igniter due to the mechanical shock of the event. Cabling and plastic component ID tags showed signs of melting damage. Most of the damage was only on the surface, but there were portions of cables where the insulation conductors were exposed. To prevent additional heat damage to cables on subsequent tests, a heat-resistant blanket was wrapped around cabling near the engine, and at locations where heat-damage was noted.

Engine performance data review for hot-fire 8 is complicated due to the large offset which occurred to the thrust measurement system. The thrust data can be analyzed by applying a different zero-offset after engine ignition. This allows a reasonable look at engine performance, but it must be realized that the load-cell uncertainty is increased and that the thrust calibration curve may have also changed. For these reasons, this data must not be relied upon to make engineering decisions, but it can provide some insight to engine performance. As is expected, engine performance

decreases as cell pressure increases (altitude is lost). The engine lit at approximately 90,000 ft of simulated altitude and dropped to about 60,000 ft when the profile was terminated.

8. Hot-Fire 9

Prior to resuming altitude hot-fire operations, the test team reviewed data and video from hot-fire 8 to determine the cause of the large fire-ball event which occurred at engine start-up. Video review supports the hypothesis that free propellant released during the start-up transient, but prior to actual ignition was rapidly dispersed into the cell due to the low ambient pressure in the test cell. Once ignition occurred, a flame propagated to the free propellant throughout the cell. In order to mitigate the start-up fire-ball observed from hot-fire 8, a new profile sequence was developed. An additional measure taken to reduce the energetic event was to not open the nitrogen break valve until after the ignition sequence. This allowed the ignition sequence to occur at a higher altitude and lower pressure of about 0.1 psia. At this pressure, the pressure resulting from a similar energetic event would be reduced by half.

The next hot-fire attempt used the same run-tank set-points and manifold temperatures as hot-fire 8 while using the torch igniter opposed to the J-2X pyrotechnic igniter. Hot-fire 9 resulted sequence-inhibited non-start due to a leak in the torch-igniter assembly. The test team proceeded to re-torque all fittings on the test manifolds. This is a significant lessons-learned: following a hard-start, all connections should be re-torqued. Finding one loose fitting should have been treated as symptomatic of a larger loose-fitting issue to improve safety and eliminate the unnecessary sequence-inhibit hot-fire 9.

9. Hot-Fire 10

Hot-fire 10 repeated the conditions for hot-fire 8 but with the new "soft-start" profile and mitigations to prevent the fire-ball seen during the start-up of hot-fire 8. The engine lit successfully and the start-up transient was much softer than hot-fire 8 in terms of force and acceleration on the engine. However, a flame-front/fire-ball was still present at start-up. After the start-up transient, the engine plume was observed as a blue-white stream with a shock a few feet under the nozzle. Figure 16 represents the fireball observed during start up.

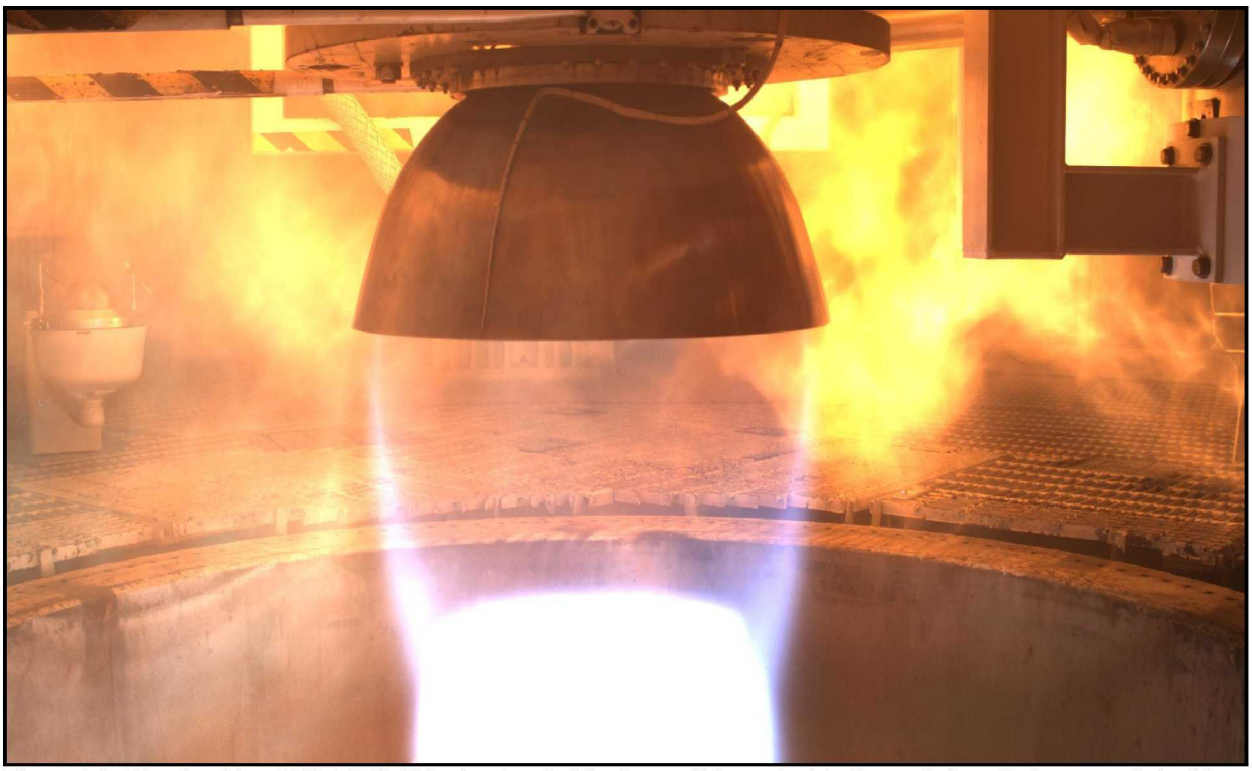

Figure 16: Hot-fire 10 at WSTF TS-401, simulated altitude conditions, dual-bell nozzle installed, gas torch ignition

The plume appears slightly under-expanded in the dual-bell nozzle. As cell pressure increased through-out the firing, the shock moved closer to the nozzle exit plane. The engine burned for approximately 18 seconds at which point the test was stopped due to high test cell ambient temperatures. Cell temperatures reached 363° F on a thermocouple located behind the 100 lb_f Service Well, and 487°F on a thermocouple located near the diffuser opening. Post test inspection revealed that insulation on the thermocouple wire had melted and exposed the wire.

In hot-fire 10, a larger altitude sweep was achieved than in the previous hot-fire 8. Due to the fire-ball observed at the start-up of hot-fire 10, the test team decided that the fire-ball mitigation techniques used were not sufficient to allow further testing of the Armadillo engine with SASS.

10. Post-Test Operations

A bore-scope was used to perform an internal inspection of the engine. No anomalies were reported and there did not appear to be any further metal erosion since earlier inspections. The high-temperature coating on the engine and nozzle surfaces was flaked off in many places. The flaking had first been noticed following the first round of ambient-pressure tests at WSTF. No direct measure of the amount of this was made. Prior to storing the engine, it was precision cleaned by the WSTF Component Services group. All engine ports were flushed and the effluent captured. The primary constituents of the engine contaminants were soot and high-temperature coating flakes. Also during the cleaning, the WSTF component Services group observed a flake of metal detaching from the exterior of the engine chamber.

D. Results and Conclusions

1. Summary

The test program met the following objectives:

- Demonstrated pyrotechnic ignition and torch igniter ignition of a cryogenic engine at altitude and ambient conditions.
- Gathered improved data on the propellant manifolds pressure drop at a variety of flow rates.
- Measured engine performance at varying mixture ratios from 1.5 to 2 at ambient and simulated altitude conditions.
- Measured engine performance during an altitude sweep, starting at ~90,000 ft and ending at ~50,000 ft.
- Measured engine performance of the Dual-bell nozzle at ambient and simulated altitude conditions during an altitude sweep.
- Provided shake-down of the APSTB for future projects. Some points that were identified as needing improvements include:
  - Dynamic water hammer effects in the test system manifold need to be reduced
  - Test system pressure drop needs improvement in order to achieve higher flow rates and test pressures
  - Free-propellant at start-up may be an issue. However, this may be a relic of running the SASS versus the LASS. The video and data review of the previous RS-18 hot-fires with LO2 / LCH4 (similar engine class) indicated the same flash and ignition delay at the start of the engine, but the LASS system was able to evacuate the unburned propellant that was expelled during the few hundred millisecond ignition delay of the main propellants. The LASS system prevented the rapidly expanding cloud of methane vapor from moving vertically into the test cell.

The test program failed to meet the following objectives:

- Demonstrate the test stands ability to support long duration engine firings. The last test fire provided a 18s duration and the goal of reaching a 180s engine duration was not achieved. However, AA has achieved test fires with the same engine at ambient conditions lasting 90 seconds in duration. Armadillo has run the same engine design in excess of 210 seconds with chamber pressures ranging from 200 psi down to 50 psi using ethanol as a fuel.
- Did not measure data on the RAO optimized nozzle extension for comparison to the dual-bell nozzle. This is due to time constraints at WSTF.
- Did not measure steady-state engine firings at a stable simulated altitude.
  - The original test matrix relied on LASS for all the simulated altitude firings, which would have provided a steady-state high-altitude simulation.
  - Although the LASS was not used, running the SASS characteristically results in an altitude sweep (due to not being able to remove the exhaust gases from the test cell fast enough). This is the first time in history a LO2 / LCH4 engine using a dual-bell nozzle while varying pressure was fired.

2. Analysis

The engine exhibits the expected behavior of decreasing thrust and efficiency as test cell pressure increases. An interesting comparison is hot-fire 3 which was performed at ambient cell pressures and at the same run-tank set-points and temperatures as hot-fire 10, which included the altitude sweep.

Calculating Isp, hot-fire 3 begins with an Isp of approximately 141s and decreases to 137s over a 4 second interval (looking at steady state only). In comparison, hot-fire 10 begins with an Isp of approximately 227s and

decreases to 133s over a 17 second interval (also only looking at steady state data). The Isp at the end of 5 seconds of steady state firing is 203s. The average calculated vacuum Isp for hot-fire 3 was 139 sec and for hot-fire 10, average vacuum Isp was calculated to be 174 sec.

Hot-fire 3 is clearly under-expanded in the Section 1 nozzle, whereas hot-fire 10 expansion at the exit due to the dual-bell nozzle is greater than the diameter of the Section 1 nozzle. As expected, the greater plume expansion in the nozzle for hot-fire 10 provides additional thrust and increased engine performance for roughly equal total mass flow rates.

However, it is still unknown how the plume expands inside the dual-bell nozzle and how that may affect the engine performance. The test was stopped before the pressure in the test cell would increase enough to show the sharp transition between Section 1 and Section 3 of the dual-bell nozzle. The increase in pressure of the test cell is a result of the hot exhaust gases from the engine and the lack of the ability to remove them from the test cell fast enough. While this allows for an altitude sweep, the temperature must be continuously monitored to avoid damage to the test cell. Due to thermal effects from the exhaust gases, it is unlikely this can ever be reproduced in a ground test configuration while firing. However, a cold flow of the engine could reproduce this separation effect and is a source for future testing.

The nozzle temperature measurements provide a clue as to how the plume might be shaped inside the nozzle. Figure 17 shows nozzle temperatures during hot-fire 10. As expected, highest temperatures generally are found at the throat region (TENG 7 to 9 and TCHAMB 1 to 3). Past the throat temperatures become lower until the end of the Section 1 nozzle is reached. Here, there is a slight rise in temperature at TCHAMB8 and TCHAMB9, the latter which is just above the weld for the mounting flange. There is a sharp drop in temperature at the dual-bell nozzle, especially later in the hot-fire profile as temperatures become more pronounced. Temperatures gradually increase further along the dual-bell nozzle, with the sharpest increase occurring at the lip.

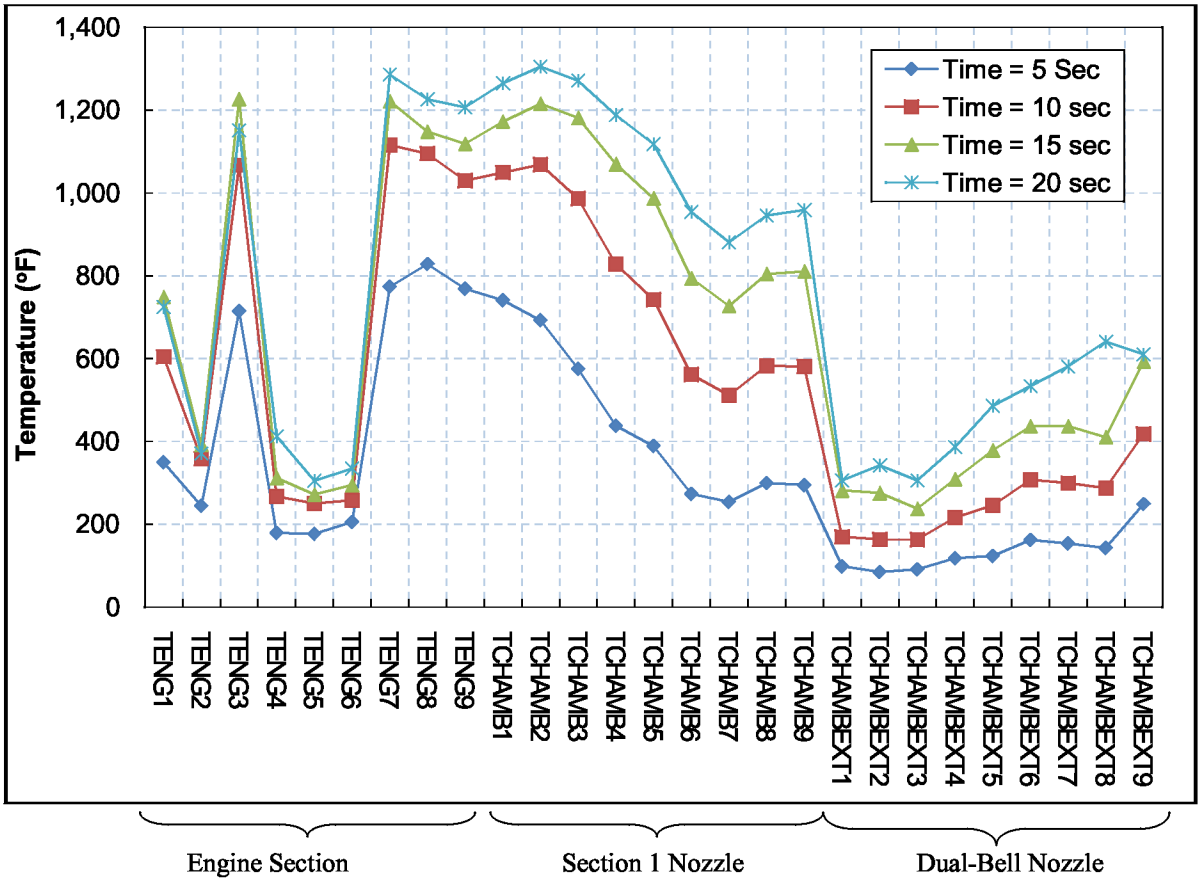

Figure 17: Hot-fire 10 Engine and Nozzle Temperatures, dual-bell nozzle configuration, simulated altitude conditions "sweep" from 90,000 ft to 50,000 ft from 0 to 20 sec.

The average flow rates, chamber pressure, and mixture ratio of each hot-fire was entered into TDK and used to calculate the theoretical Isp, thrust, and C* efficiency. In order to calculate the mixture ratio of each of the two zones in TDK, the mass percentage of fuel flowing through the fuel film cooling holes was calculated based on the geometry of the like impinging fuel holes versus the fuel film cooling holes on the injector plate. A surface effect loss was assumed due to the fact the fuel film cooling holes are significantly larger than the like impinging fuel holes. The estimated film cooling mass flow percentage was then multiplied by the measured fuel flow rate from the hot-fire runs in order to calculate the actual fuel film cooling mass flow rate in zone 2. The mass flow rate percentage of the two zones was then calculated based on the measured total mass flow rate in each hot-fire. A fuel rich mixture ratio was assumed in the fuel film cooling region and the mixture ratio in zone 1 was calculated based on the average total mixture ratio measured in each hot-fire. For hot-fires 1 to 7, the contour of the Section 1 nozzle was used based on video feed of the plume. For hot-fires 8 to 10, the Rao optimized nozzle contour was used. While the actual test at altitude used the full contour of dual-bell nozzle, TDK was unable to converge with the inflection point required to ensure a sharp transition in the dual-bell. For this reason, the data calculated is for informational purposes only. The theoretical Isp and thrust in TDK should be higher based on a larger area expansion ratio (making the efficiencies calculated lower). However, the C* calculation is independent of the nozzle and an accurate comparison.

Based on assumptions above, the average Isp, thrust, and C* efficiency at ambient pressure for hot-fires 2 thru 7 is 49%, 62%, and 79% respectively. The average Isp, thrust, and C* efficiency at altitude for hit fires 8 and 10 is 61%, 77%, and 79% respectively. Returning to the previous comparison of hot-fire 3 versus hot-fire 10, the Isp and thrust efficiency is slightly improved at altitude while the C* is for the most part, unaffected. It is important to note that engine stability and reliability, not optimized performance, is the goal of this engine design.

V.Appendices

A. Appendix B: Performance Plots

1. *Hot-fire 3 Plot: Performance Data*

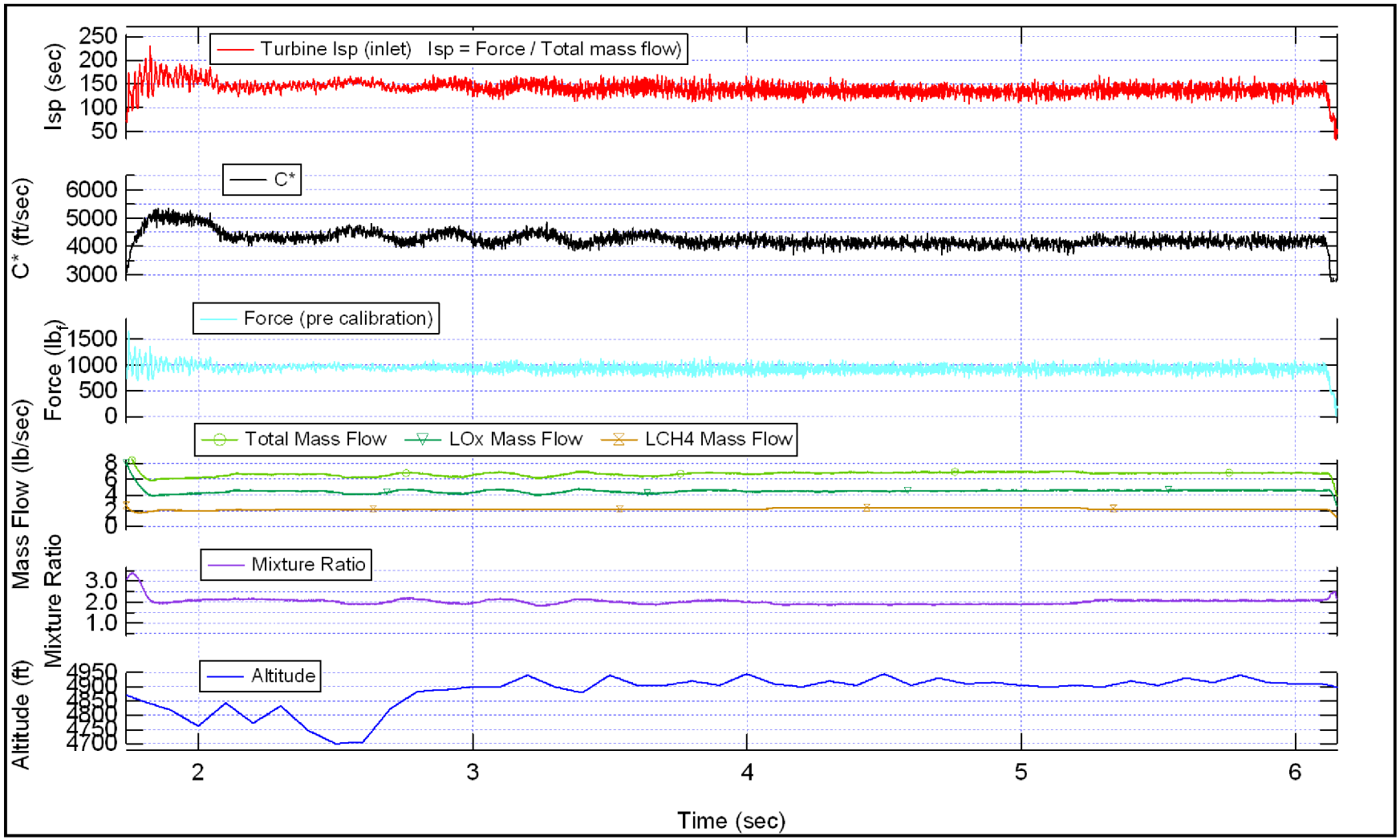

2. *Hot-fire 10 Plot: Performance Data*

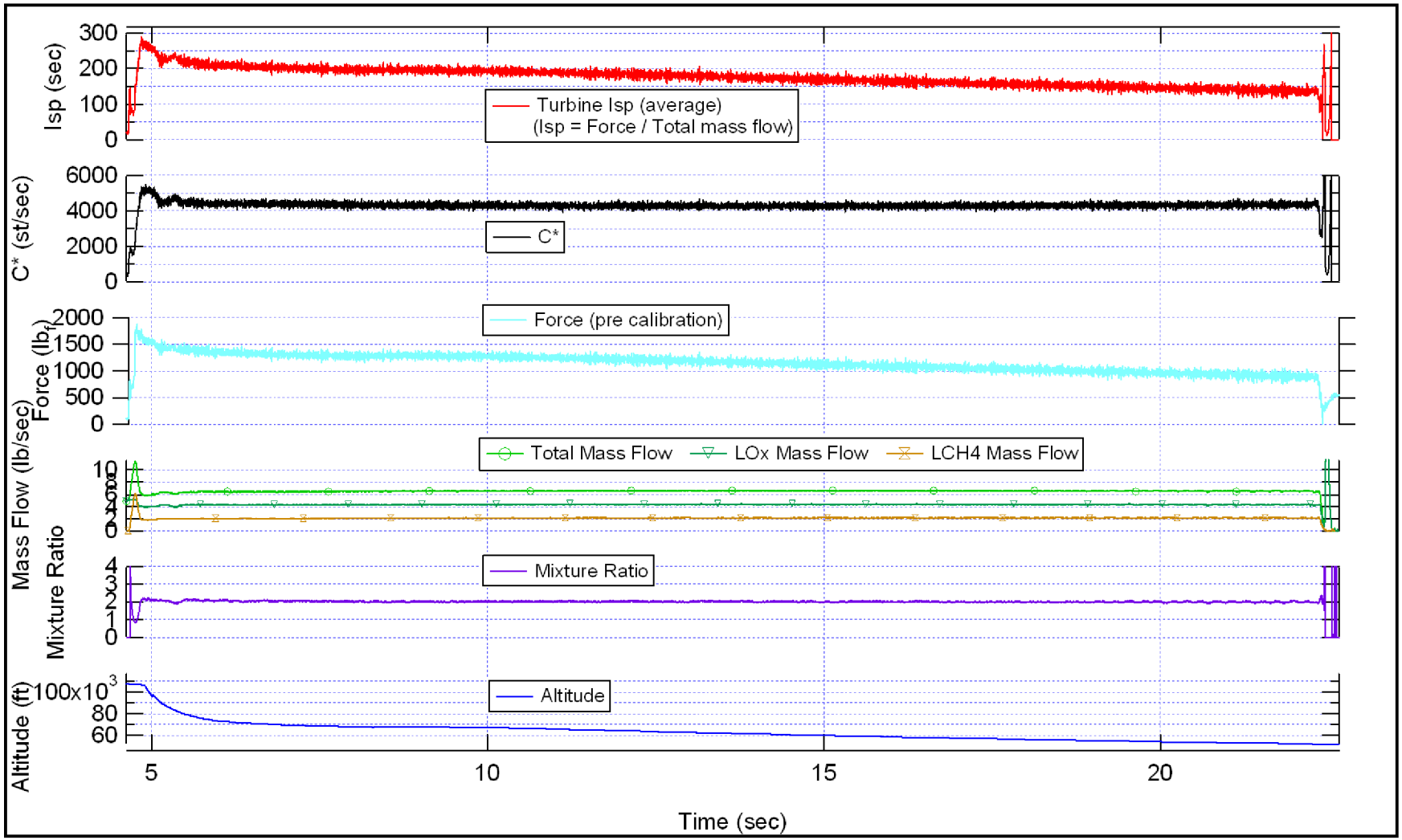

3. *Hot-fire 10 Plot: Thermocouple Data*

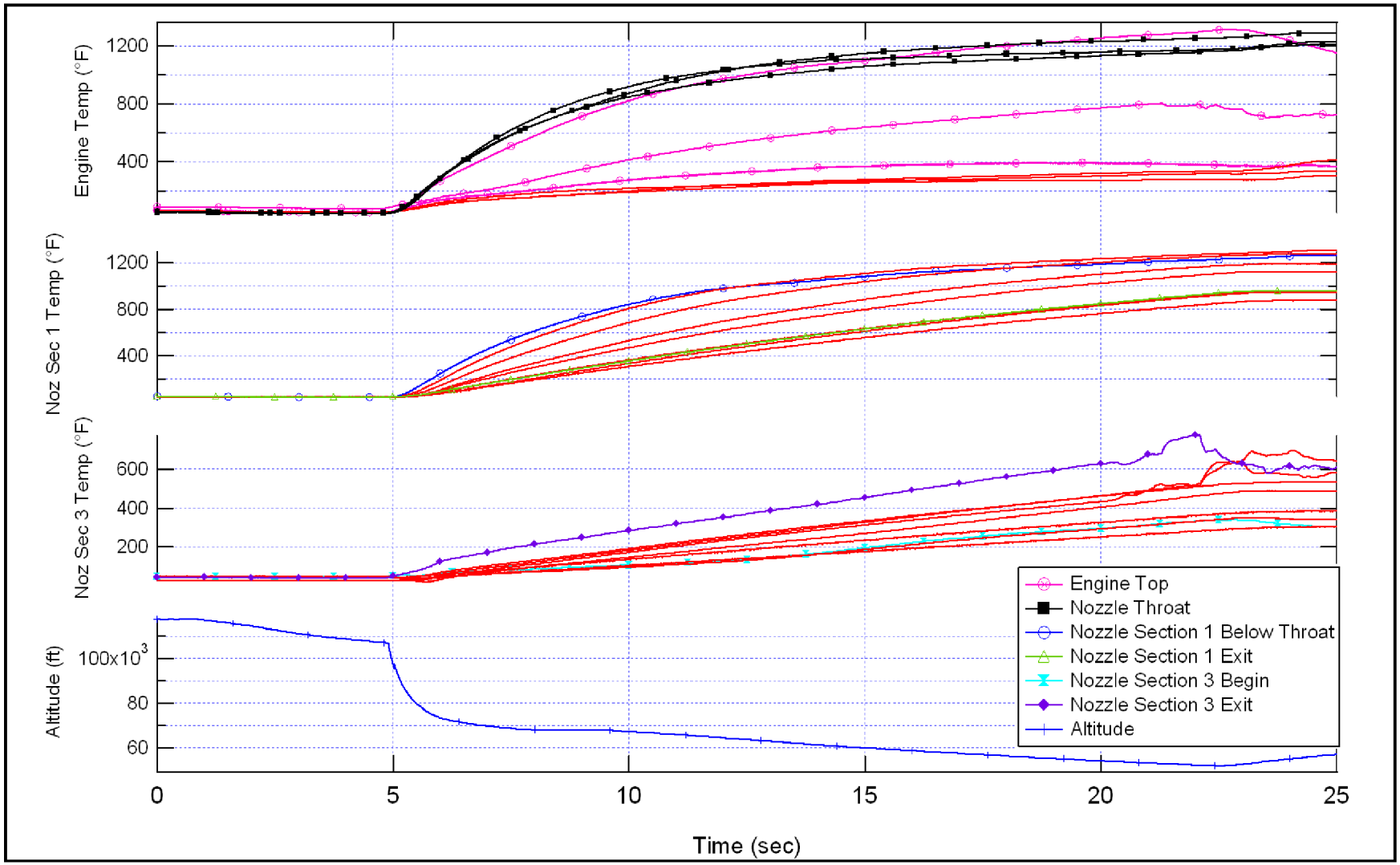

4. Hot-fire 10 Plot: Injection Pressure

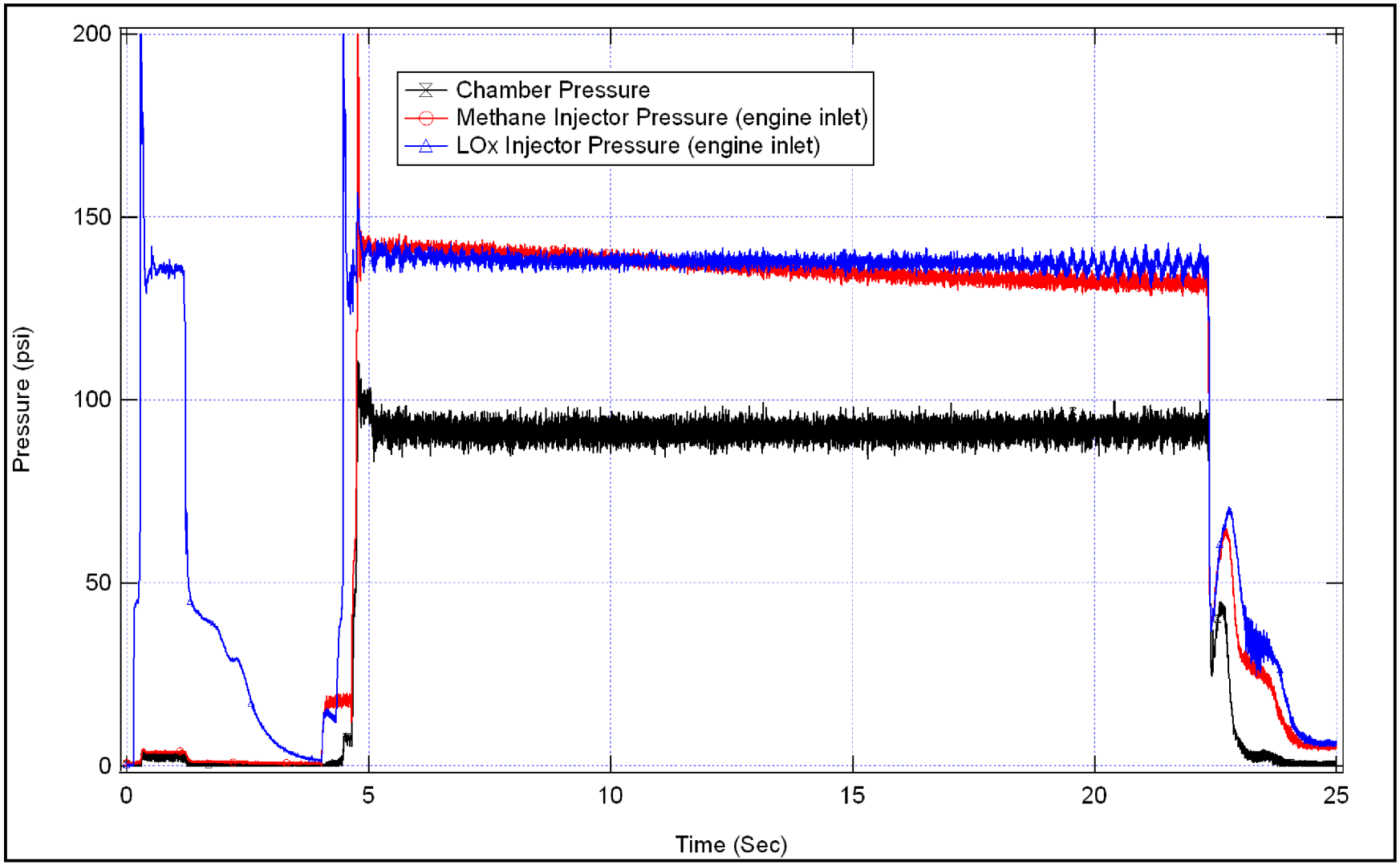

5. *Hot-fire 10 Plot: Chamber Pressure*

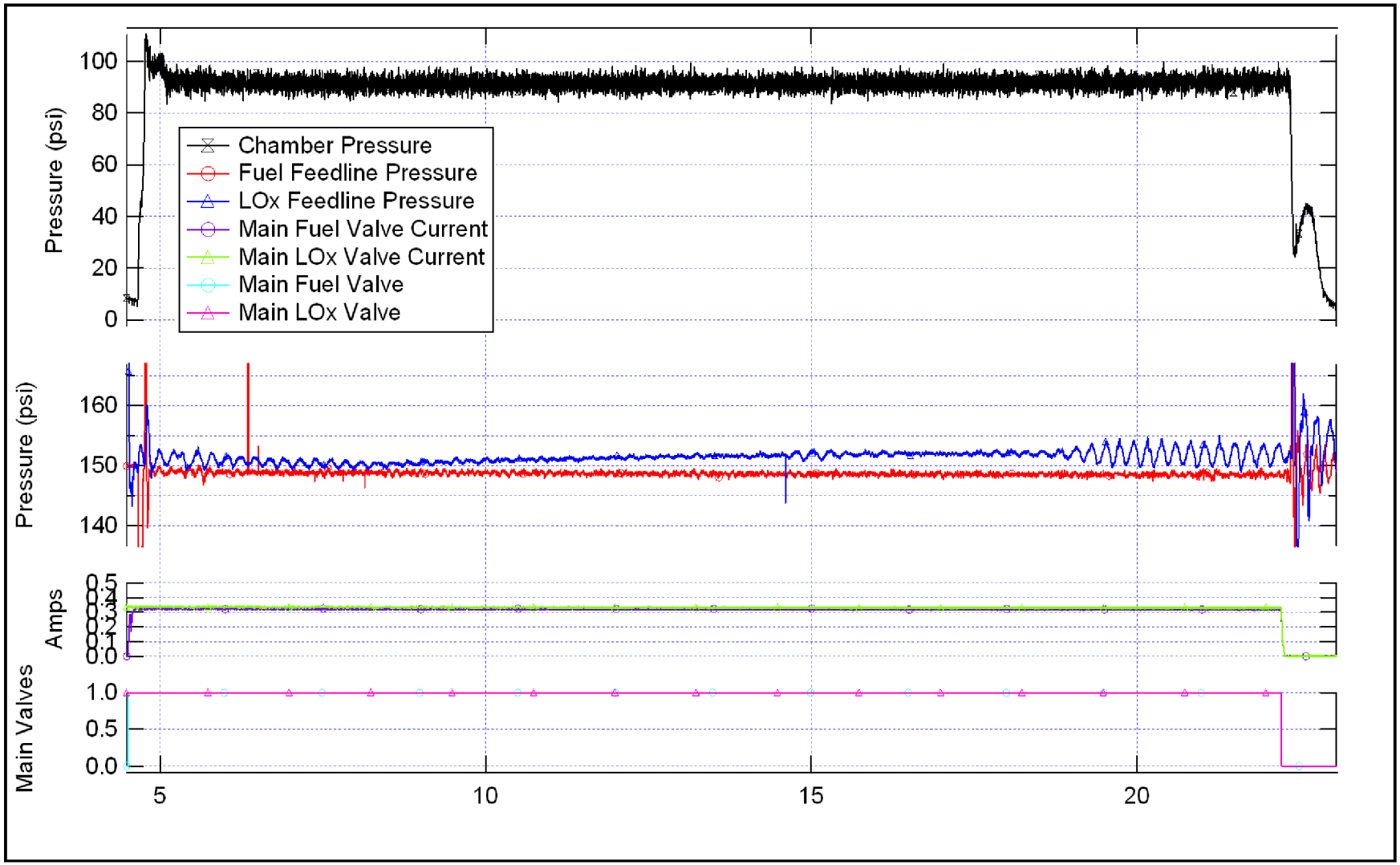

VI.References

1. Otsu, H., Miyazawa M., Nagata Y., "Design Criterion of the Dual-Bell Nozzle Contour", IAC-05-C4.2.08, Oct., 2005.
2. Nickerson, G. R., Dang, L. D., Coats, D. E., "Engineering and programming manual Two-dimensional kinetic reference computer program (TDK)", NASA-Ch-1786, April 1985.
3. Hagemann, G., Immich, H., "Rocket Engine Nozzle Concepts," Liquid Rocket Thrust Chambers: Aspects of Modeling, Analysis, and Design, Vol 200, pp. 437-467.
4. Frey, M., and Hagemannt, G., "Critical Assessment of Dual-Bell Nozzles," *Journal of Propulsion and Power*, Vol. 15, No. 1, January-February 1999.
5. Miyazawa M., Otsu, H., "An Analytical Study on Design and Performance of Dual-Bell Nozzles," AIAA Paper 2004-3080, Jan., 2004.
6. Emerson Process Management Flow, "Applicability of Coriolis Technology for Cryogenic Service Using Micro Motion Coriolis Meters for LNG Allocation Metering", Sept. 2004.
7. Horn, M., and Fisher, S., "Dual-Bell Altitude Compensating Nozzles," NASA-CR-194719, 1994.